

## MODELING AND ANALYTICAL STUDY FOR EFFICIENCY IMPROVEMENT FOR THIN FILM SOLAR CELLS BASED ON CdS/PbS, CdS/CdTe, AND CdS/CdSe

R. A. SABORY-GARCIA\*, A. L. LEAL-CRUZ, A. VERA-MARQUINA,  
L. A. GARCÍA-DELGADO, A. GARCÍA -JUAREZ,  
A. G. ROJAS-HERNANDEZ

*Department of Physics Research, University of Sonora, P.O. Box 5-088, ZIP code 83000, Hermosillo, Sonora, México*

A theoretical modeling is developed under the theory of Sah Noyce in order to analyze, understand and predict the behavior of heterostructure solar cells. The cell is mainly based on 4 stacked films: glass, ITO, CdS, active layer, and back contact. The presented study is focused on using the optical and electrical analysis to determine which involved parameters are the most critical for efficiency improvement. Considered parameters are depletion region, donor and acceptors' concentrations and effective layer thickness. The ultimate efficiency of the cell is calculated using a Mathematical Modeling System (MMS) developed on Matlab. Using the MMS the quantum efficiency is also obtained and studied. The thickness for the effective layer varies from 0.5 to 2 $\mu$ m. For the MMS, three active layers cases were studied: PbS, CdTe, and CdSe. Ultimate efficiency obtained was 10.24, 5.69, and 6.33%, respectively. Standard solar spectra ASTM G-173-03 (International standard ISO-9845-1-1992) was used, under conditions of AM 1.5 direct.

(Received September 21, 2018; Accepted December 13, 2018)

*Keywords:* Heterostructure, Tandem, Solar-Cell, CdS, CdTe, CdSe

### 1. Introduction

An increase of solar cell efficiency has been reported recently [1,2,3,4,5]. Ultimate efficiency is calculated assuming a quantum efficiency of 1 corresponding to energies greater than the band gap. Likewise, the solar cell is considered as a perfect black body with no radiative recombination.

Through this research a comparative study is driven in order to determine the theoretical ultimate total efficiency. The study corresponds to an analytical (theoretical) comparison of 3 different semiconductor materials corresponding to the II-VI and IV - VI groups. These results are compared to reported researches by different authors, obtaining similar behaviors. A CdS layer is used as a window with three different materials with different bandwidths and different extinction coefficients. The above materials are: lead sulfide (PbS), cadmium telluride (CdTe), and cadmium selenide (CdSe). These three materials are used as active layers. Multi-Reflection was considered across all the layers, and the absorption was taken into account in the ITO/CdS junction for all three layers. Figure 1 illustrates the structure modeled through this paper.

PbS was selected since it is a semiconductor with a narrow bandgap and has the ability to absorb energy near infrared. Likewise, CdTe is used as an absorber layer since it has quasi optimal absorption characteristics (around 90%). Lastly, CdSe was chosen given its physical and chemical properties.

One of these properties corresponds to the range where CdTe's band gap falls, matching the solar energy spectrum. In addition, CdTe is capable to adjust the energy level through quantum dots.

---

\* Corresponding author: rafael.sabory@unison.mx

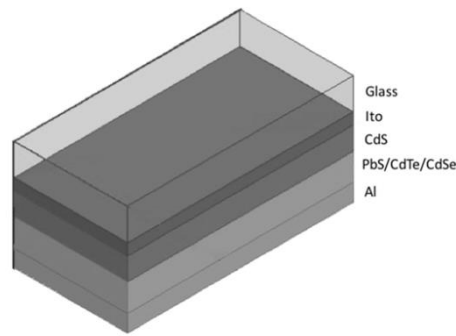


Fig. 1. Thin film solar cell modeled on the MMS. The solar cell is composed by glass, a front contact layer ITO, a window layer CdS, (n type), an active layer which is replaced for each case PbS, CdTe or CdSe (p type), and a back contact layer of Aluminum (not considered on computations).

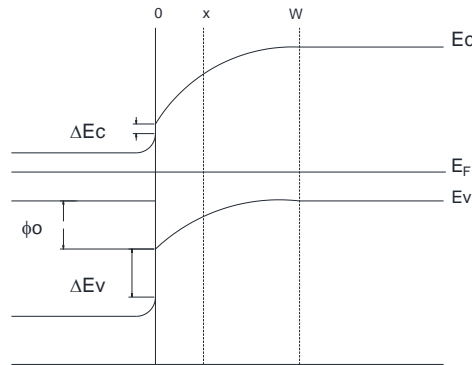


Fig. 2. Energy band diagram for the PbS, CdTe and CdSe layers.

Fig. 2 represents the energy band diagram for all three active layer materials. In the last mention figure, conduction ( $E_C$ ), Fermi energies ( $E_F$ ), valence energies ( $E_V$ ), barrier height ( $\phi_0$ ), and space charge region ( $W$ ) are shown.

## 2. Theory and modeling

The presented analysis is based on the Sah, Noyce, and Shockley theory of carrier generation and recombination in P-N structures [6]. The theory behind optical and electrical parameters required for the modeling is described in the next paragraphs.

### 2.1 Optical parameters

In order to estimate the transmission spectrum it is needed to know the total transmittance for the given number of layers. Transmittance can be defined as the ratio of the intensities of the emergent and incident beams of light [7]. In a same manner, the whole structure is characterized by the reflection coefficient ( $R$ ), the absorption coefficient ( $\alpha$ ), the complex reflection coefficient and the thickness ( $d$ ) of layers.

The absorption coefficient  $\alpha$  is related to the extinction coefficient  $k$ , as well as, to the wavelength by:

$$\alpha = \frac{5\pi k}{\lambda} \quad (1)$$

In a solar cell, the light is absorbed by the material when the energy of light is greater than the material band gap energy [8]. In practical cases, semiconductors have impurities which generally can present absorption during characterization. Under the above circumstances, the transmittance is determined by:

$$T = \frac{(1 - R)^2 e^{-\alpha d}}{1 - R^2 e^{-2\alpha d}} \quad (2)$$

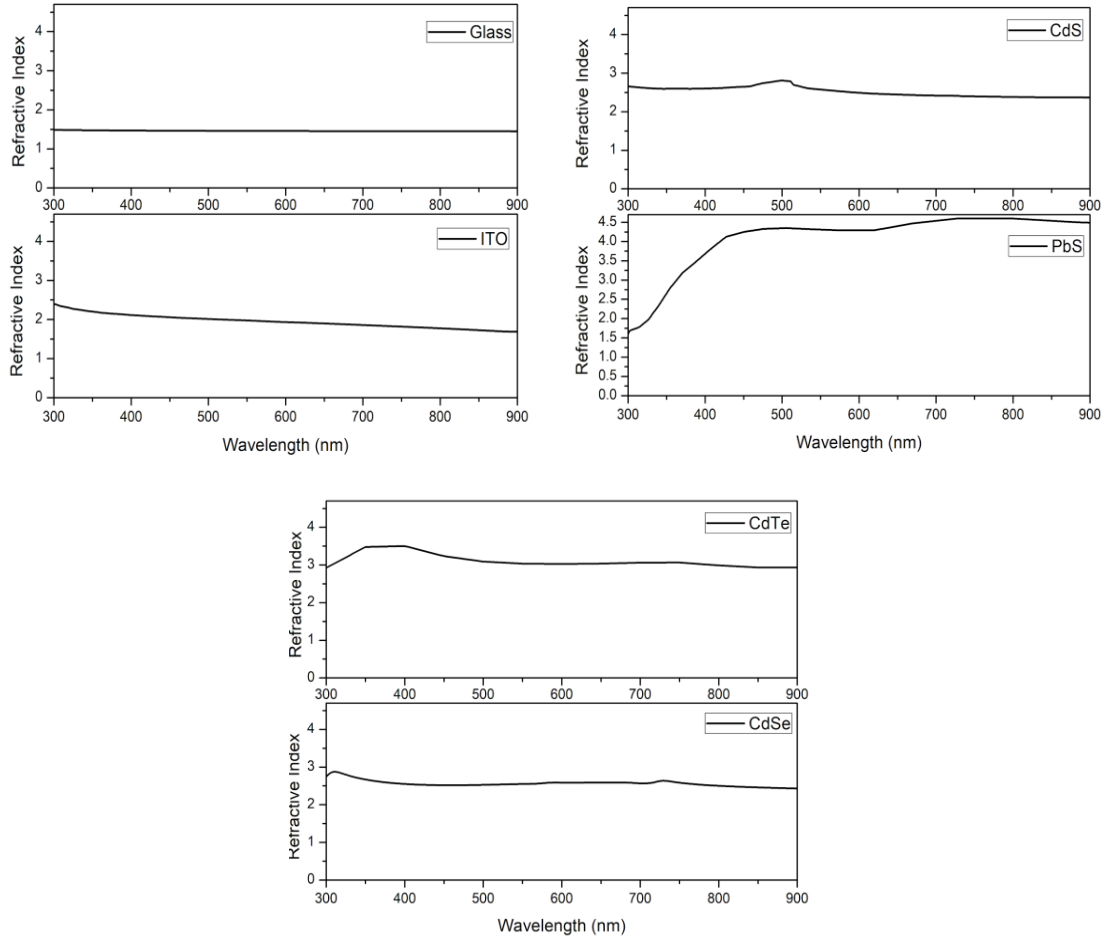


Fig. 3. Refractive index for Glass, ITO, CdS, PbS, CdTe and CdSe used for the presented model.  $n$  is considered within the range of study, from 300 to 900 nm [9, 10, 11].

Based on the Fresnel theory [8], when light has an incidence about the normal vector and considering the imaginary index refraction term, the reflection at the boundary of two media can be computed using Equation (3):

$$R = \frac{(n_1 - n_2)^2 + (k_1 - k_2)^2}{(n_1 + n_2)^2 + (k_1 + k_2)^2} \quad (3)$$

where  $n_1$  and  $n_2$  are the refractive indices of the two media. While,  $k_1$  and  $k_2$  are the extinction coefficient for the same two media. The values for  $n$  and  $k$  used through this where taken from [9, 10, 11] and can be observed in Fig. 3 and Fig. 4.

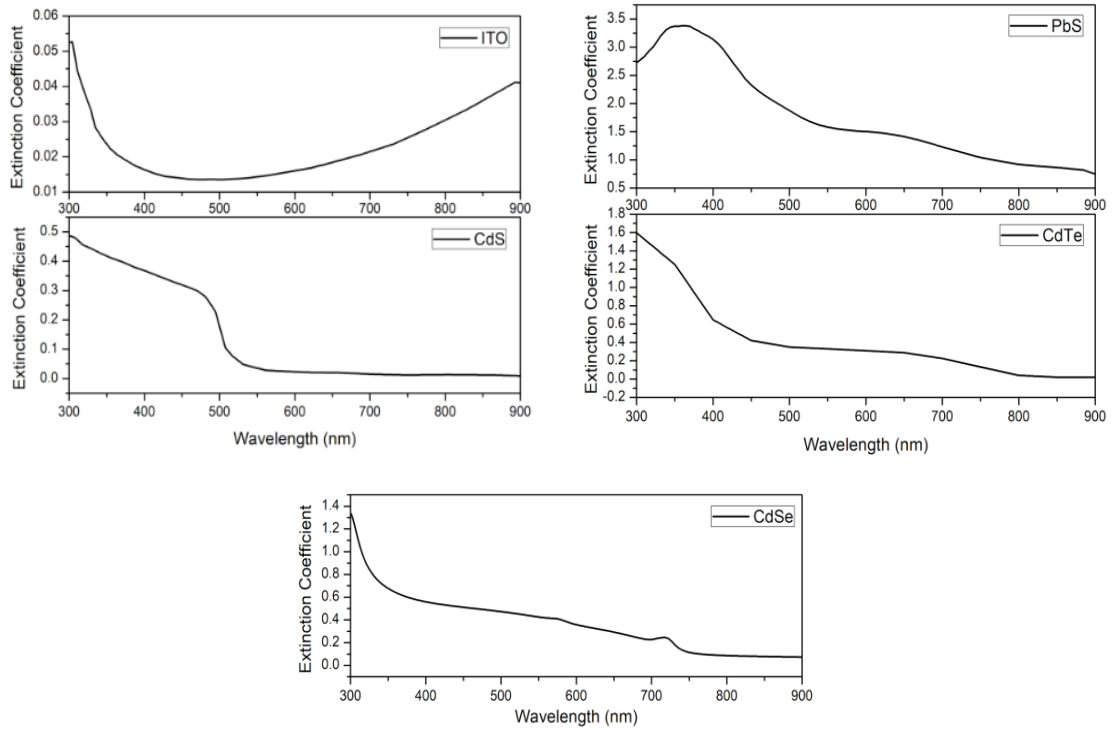


Fig. 4. Extinction coefficient for ITO, CdS, PbS, CdTe and CdSe used for the presented model. For this case,  $k$  for glass was considered constant and equal to 0. [9, 10, 11].

For a multilayer structure, the light transmitted up to the absorber layer through all reflections can be determined by:

$$T(\lambda) = (1 - R_{j,k})(1 - R_{j+1,k+1})(1 - R_{j+2,k+2})(1 - R_{j+3,k+3}) \quad (4)$$

The absorption coefficient ( $\alpha$ ) will be taken into account for the CdS and ITO layers. Thus, the transmission coefficient ( $T(\lambda)$ ) corresponding to multiple reflections can be computed using Equation (5):

$$T(\lambda) = (1 - R_{j,k})(1 - R_{j+1,k+1})(1 - R_{j+2,k+2})(1 - R_{j+3,k+3})(e^{-\alpha_j d_j})(e^{-\alpha_{k+1} d_{k+1}}) \quad (5)$$

where  $\alpha_j$ ,  $d_j$ ,  $\alpha_{j+1}$ , and  $d_{k+1}$  correspond to the absorption coefficient and layer thickness for the front contact (ITO) and windows layer (CdS) respectively. The used thickness for ITO and CdS layers were 150  $\mu\text{m}$ .

Once the transmittance is known, it is necessary to determine the space charge region (or depletion layer) denoted as  $W$ . When light impinges the junction between the window layer and the active layer, it knocks an electron off the n-type material atom and it creates an electron-hole pair.  $W$  is highly related to the difference of donor and acceptor concentrations, as it can be seen in Equation (6).

$$W = \sqrt{\frac{2\epsilon_r \epsilon_0 (\Phi_0 - qV)}{q^2 (N_a - N_d)}} \quad (6)$$

In Equation (6),  $\epsilon_r$  and  $\epsilon_0$  stand for the active layer relative dielectric constant and permittivity for vacuum, respectively. Even though, the dielectric constant varies with the frequency, for PbS, CdTe, and CdSe values for  $\epsilon_r$  were fixed. The applied numbers for  $\epsilon_r$  were: 17.2 for PbS, 10.16 for CdTe and 9.5 for CdSe [12, 13, 14].

From Fig. 5, it can observe that the behavior for CdSe and CdTe are similar, given that the dielectric constants don't differ from each other in great manner.

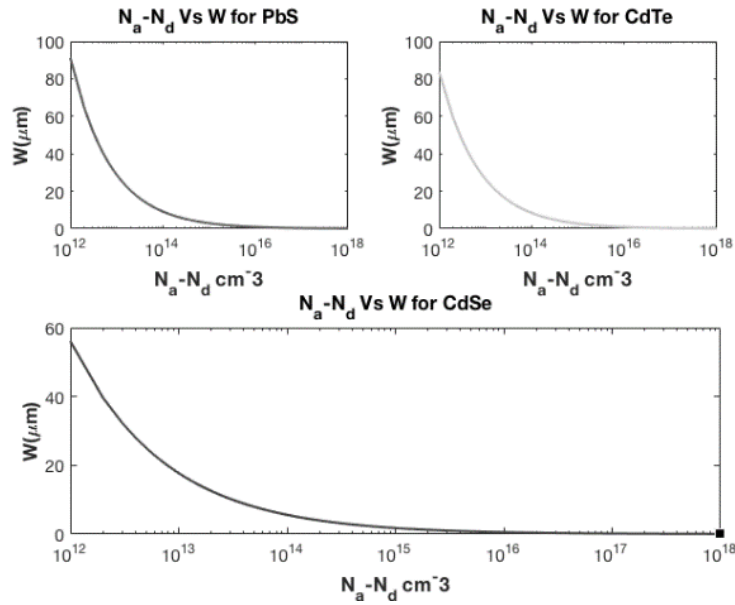


Fig. 5. Concentration of uncompensated donor and acceptor in the window and active layers. The range goes from  $10^{12}$  to  $10^{18}$ .

When designing a solar cell, it is looked forward to delay or avoid, as much as possible the recombination process by increasing the collection of carriers. From Figure (5), it can be seen that as the concentration of uncompensated donor and acceptors arises,  $W$  is decreased and in consequence the quantum efficiency does too. This behavior can be attributed to the absorption of a large quantity of photons outside the depletion layer during the drift process.

The quantum efficiency (QE) corresponds to the ratio between the produced electrons on the cell circuit and the number of incident photons. The internal QE is calculated in the junction between the CdS layer and the active material layer (PbS, CdTe and CdSe). IQE is composed by two components: the drift component and the diffusion component. The drift component happens when an electron-hole pair is generated in the depletion layer, while the diffusion component occurs when a pair of electron and hole is achieved in the neutral region of the active layer.

The diffusion and drift component can be calculated using the following equations [15]:

$$\eta_{drift} = \frac{1 + \frac{S}{D_n} \left( \alpha + \frac{2}{W} \frac{\phi_0 - qV}{kT} \right)^{-1}}{1 + \frac{S}{D_n} \left( \frac{2}{W} \frac{\phi_0 - qV}{kT} \right)^{-1}} - \exp(-\alpha W) \quad (7)$$

and

$$\eta_{diff} = \frac{\alpha L_n}{\alpha^2 L_n^2 - 1} e^{-\alpha w} \times \left\{ \alpha L_n - \frac{\frac{S_b L_n}{D_n} \left[ \cosh\left(\frac{d-W}{L_n}\right) - e^{-\alpha(d-w)} \right] + \sinh\left(\frac{d-W}{L_n}\right) + \alpha L_n e^{-\alpha(d-w)}}{\frac{S_b L_n}{D_n} \sinh\left(\frac{d-W}{L_n}\right) + \cosh\left(\frac{d-W}{L_n}\right)} \right\} \quad (8)$$

where  $S$  is the surface recombination velocity,  $D_n$  is the diffusion coefficient,  $\alpha$  is the absorption coefficient,  $W$  is the space charge region,  $\phi_0$  is the barrier height,  $q$  is the electron charge,  $V$  is the applied voltage,  $k$  is the Boltzman constant, and  $T$  is the temperature in Kelvin. For equation (8),  $S_b$  is the back surface recombination time on the active layer,  $L_n$  is electron the diffusion length and  $d$  is the thickness of the Pbs, CdTe or CdSe layer.

The diffusion length is then calculated using the following equation:

$$L_n = \sqrt{\tau_n D_n} \quad (9)$$

here,  $\tau_n$  is the electron lifetime. Thus the quantum efficiency can be determined by the summation of the two components as follows:

$$\eta_{int} = \eta_{drift} + \eta_{int} \quad (10)$$

The values used for this study can be seen in Table 1. Once the quantum efficiency is known, the ultimate efficiency can be determined.

Table 1. Parameter setting for the mathematical model simulator.

Parameters	Materials			
	PbS	CdTe	CdSe	Units
$E_g$	1.32	1.8	1.7	eV
$\epsilon_r$	17.2	10.16	9.5	-
$\phi_0 - qV$	0.7	1	0.48	eV
Na-Nd	$10^{18}$	$10^{18}$	$10^{17}$	$\text{cm}^{-3}$
W	0.28	0.26	0.56	$\mu\text{m}$
S	$10^7$			cm/s
$D_n$	25.8	25	5.5	cm/s
$S_b$	$10^7$			cm/s
T	300			K
$T_n$	$10^{-9}$			s
$T_p$	$10^{-9}$			s
$m_0$	$9.1093 \times 10^{-31}$			Kg
$m$	0.25	0.119	0.11	Kg
$n_i$	$10^{10}$			$\text{cm}^{-3}$

## 2.2 Electrical parameters

As a means to obtain the ultimate efficiency, behavior of a solar cell can easily be represented as pn diode. Thus, one can obtain the I-V curve from the equation corresponding to the electric model represented on Fig. 6. I-V curve is formed by overlapping the characteristic curve of a diode in the dark and the curved formed once the light generates the current through the circuit [16]. Once the cell is illuminated by solar light it adds current to the existing dark currents. The above phenomenon is described by the following equation:

$$I = I_L - I_0 \left[ \exp\left(\frac{qV}{nkT}\right) - 1 \right] \quad (11)$$

where,  $I_L$  is the light generated current,  $I_0$  is the dark saturation current, and  $n$  is the ideality factor. Equation (11) represents the current of an ideal solar cell. Usually for a solar cell, this curve is expressed in terms of current density  $J(\text{A}/\text{cm}^2)$ .

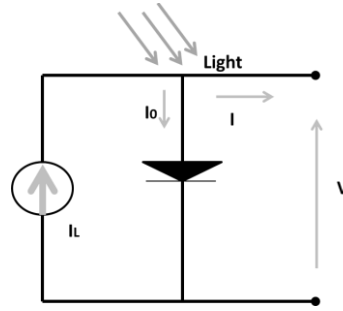


Fig. 6.- Electric circuit model for a solar cell.

To obtain a more accurate computation for the J-V curve on a solar cell, several parameters are taking into account, such as transmittance, solar irradiance, quantum efficiency, short circuit current, and the open voltage circuit.

Short circuit current density ( $J_{sc}$ ) can be considered as one of the main parameters to model and characterize a solar cell.  $J_{sc}$  can be calculated as follows:

$$J_{sc} = q \sum_i T(\lambda) \frac{\phi_i(\lambda_i)}{h\nu_i} \eta(\lambda_i) \Delta\lambda_i \quad (12)$$

where,  $T(\lambda)$  is the optical transmission spectrum across the layers of the CdS structure,  $\phi_i$  is the spectral radiation power density,  $\eta$  is the quantum efficiency,  $\Delta\lambda$  is the value between two neighbor wavelengths, and  $h\nu$  is the photon energy. As the light impinges into the solar cell, the J-V curve can be moved to the fourth quadrant were the power can be extracted. In this particular case, the standard solar spectra ASTM G-173-03 (International standard ISO 9845-1 1992) was used, under conditions of AM 1.5 direct.

The function of the J-V curve can be represented as:

$$J(V) = J_d - J_{ph} \quad (13)$$

where,  $J_d$  is the dark current density and  $J_{ph}$  is the current density generated as a result of the photovoltaic effect (for this case  $J_{ph}=J_{sc}$ ). According to the theory of generation and recombination of Sah-Noyce-Shockley, the generation-recombination rate in the distance  $x$  of the depletion layer is a parameter that must be considered at the moment to compute  $J(v)$ . Since, it is directly attached to the recombination generation current. This generation-recombination rate is denoted by  $U$  and is:

$$U(x, V) = \frac{n(x, V)P(x, V) - n_i^2}{\tau_{p0}[n(x, V) + n_1] + \tau_{n0}[P(x, V) + P_1]} \quad (14)$$

where,  $n(x, V)$  and  $P(x, V)$  are the carrier concentration in the conduction and valence bands respectively. While,  $n_i$  is the intrinsic carrier concentration,  $\tau_{p0}$ , and  $\tau_{n0}$  are the hole and the electron effective lifetime.  $n_1$  and  $p_1$  are obtained from the energy between the valence band and the generation-recombination level.

As reported by Sah Noyce [6], for conditions when exist a large reverse bias,  $-q(\Phi_p - \Phi_n)/kT \gg 1$ , an approximation for  $U$  can be applied, due to the recombination rate can be considered as a constant over the transition region and the hole current obtain a proportional dependency to the distance. Thus, equation (14) can be substituted by equation (15):

$$-U = n_i \left[ 2\sqrt{\tau_{p0}\tau_{n0}} \cosh\left(\frac{E_t - E_i}{kT} + \frac{1}{2} \ln \frac{\tau_{p0}}{\tau_{n0}}\right) \right]^{-1} \quad (15)$$

Equation (15) marginally overestimates the recombination generation current since  $U$  drops to zero near the depletion layer end. Hence, the recombination generation current considering this approximation is:

$$J_{rg} = qUW \quad (16)$$

The electron current ( $J_e$ ) across the window layer and the active layer can be analogous compared to the phenomena occurring in a pn diode, so a variation of Equation (11) can be developed considering the concentration of electrons in the bulk region of the p-active layer (PbS, CdTe, or CdSe) resulting as follows:

$$J_e = q \frac{n_p L_n}{\tau_n} \left[ \exp\left(\frac{qV}{kT}\right) - 1 \right] \quad (17)$$

and

$$n_p = N_c \exp\left(-\frac{E_g - \Delta\mu}{kT}\right) \quad (18), \quad N_c = 2 \left(\frac{m_n kT}{h^2}\right)^{3/2} \quad (19)$$

where,  $n_p$  is the electron concentration in the p-layer (active),  $N_c$  is the effective state density corresponding to the conduction band,  $E_g$  is the energy gap of the active layer,  $\Delta\mu$  is the space between the Fermi level, and the peak of the Valence band of PbS, CdTe and CdSe layers.  $m_n$  is the effective mass of the electron. In this way,  $J_d$  is obtained from:

$$J_d = J_{rg} - J_e \quad (20)$$

To obtain the maximum power of the CdS/PbS, CdS/CdTe, and CdS/CdSe solar cells, the fill factor (FF) parameter must be known. The FF is defined as the ratio of maximum power and the product of  $V_{oc}$  by  $J_{sc}$ . The FF is a magnitude related to the ultimate efficiency of conversion and can be calculated using:

$$FF = \frac{V_{mp} J_{mp}}{V_{oc} J_{sc}} \quad (21)$$

In Equation (21),  $V_{mp}$  and  $J_{mp}$  are the maximum voltage and the maximum current density respectively. While,  $V_{oc}$  is the open circuit voltage and  $J_{sc}$  is the short circuit current density. FF is usually settled from the J-V curve for each CdS material junction.

Finally, the ultimate efficiency of the solar cell is computed using equation (22):

$$\eta = \frac{V_{oc} J_{sc} FF}{P_{in}} \quad (22)$$

where  $P_{in}$  is the power input of the solar cell. The ultimate efficiency of a solar cell can be seen as the fraction of input power transformed into electricity.

### 3. Results

Fig. 7 shows the Spectrum transmission for each one of modeled cases using the MMS and Eq. (1)–(5). Figure one indicate that the range for the spectrum transmission, considering only the reflection, goes from 0.87 to 0.93. Once the absorption is taken into account, the reflection drops considerably in the wavelength from 300 to 550 nm. This value goes down to 0.20 at 300 nm. Results denote that a considerable portion of the solar cell efficiency loss corresponds to the absorption at the front contact layer and the window layer. The absorption effect can be reduced if the thickness of the ITO and the CdS layer ( $d_1$  and  $d_2$ ) is reduced [17]. For this study, 150 nm were selected for  $d_1$  and  $d_2$  since the fabrication process get more complex as these thicknesses get lower.

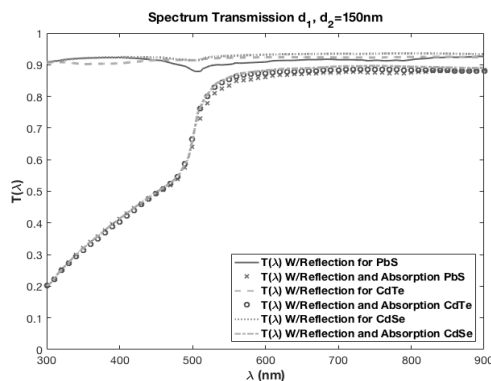


Fig. 7. Spectrum Transmission up to the active layer for the three cases (PbS, CdTe, and CdSe) where  $d_1$  and  $d_2$  is the thickness of the front contact layer (ITO) and thickness of the window layer respectively.

For the estimation of the internal quantum efficiency, Eq. (7) and (8) were considered. Fig. 8 (a) shows the drift component for the model CdS/PbS at different PbS layer with thickness in the range of 0.5 to 2  $\mu\text{m}$ . Figure 8 shows that the diffusion component can be controlled as the active layer thickness grows, corresponding to a maximum of 0.44% at 800 nm at  $d=2\ \mu\text{m}$  and a minimum of 0.02% at 340 nm and  $d=0.5\ \mu\text{m}$ . In Fig. 8 (b) it can be seen that the efficiency corresponding to the drift component varying the depletion layer distance. The values for  $W$  are selected from the results shown in Fig. 5. It can be observed that as  $W$  gets longer the drift component gets closer to 1, attributed to a larger length  $W$ , the electromagnetic field gets more intense leading into the excitation of multiple electrons as a single photon is absorbed by the cell. For this CdS/PbS model,  $W$  was fixed at 0.28  $\mu\text{m}$  and the values required for Eq. (7) and (8) are in Table 1.

In a similar way, Fig. 9 (a) shows the diffusion and the drift b) components for the simulated CdS/CdTe model. The maximum value for the diffusion component is 0.54 with  $d=2\ \mu\text{m}$  and  $W$  was fixed at 0.26  $\mu\text{m}$ .

Finally, Figure 10 represents the components of the internal quantum efficiency for the structure corresponding to the CdS/CdTe. As mentioned, the diffusion component a) gets greater values as the thickness of the active layers keep growing;  $W$  was set to be 0.56  $\mu\text{m}$ .

Once the two components were determined for each case, the internal quantum efficiency was computed making use of equation (10), and then was proceeded to obtain the electrical parameters.

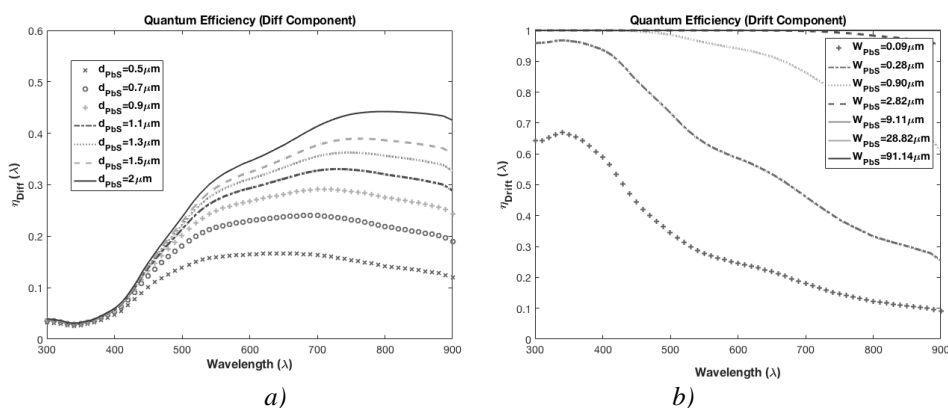


Fig. 8. Diffusion a) and Drift b) components for the solar cell model CdS/PbS. The value for  $W$  was fixed at 0.28  $\mu\text{m}$  in order to estimate the diffusion component. The figure shows the internal quantum efficiency parameters in a range from 300 to 900 nm, showing better results when there is an active layer thickness of 2  $\mu\text{m}$ .

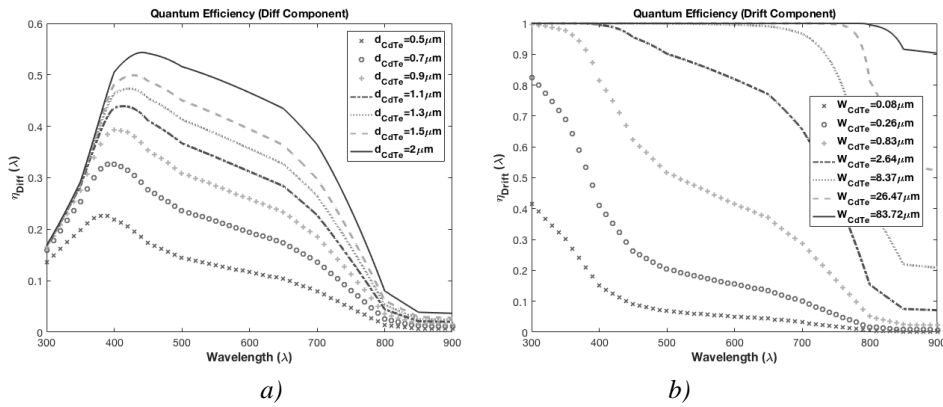


Fig. 9. Diffusion a) and Drift b) components for the solar cell model CdS/CdTe. The value for  $W$  was fixed at  $0.26\mu\text{m}$  in order to estimate the diffusion component. A better efficiency is denoted when the thickness of the active layer gets a larger value.

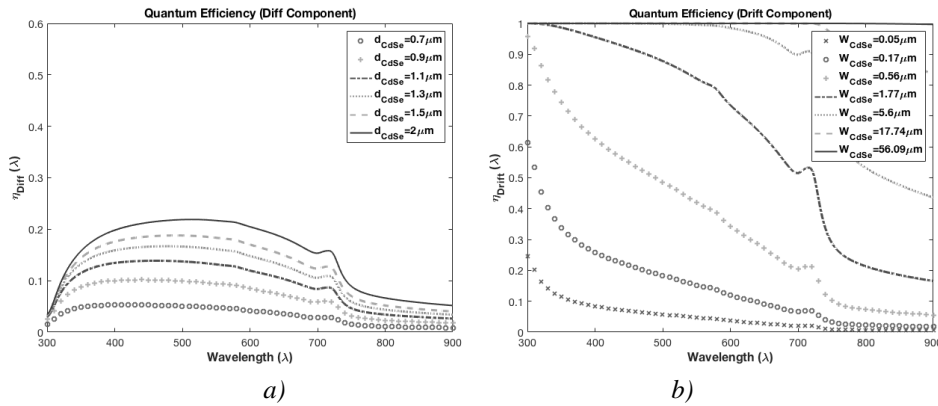


Fig. 10. Diffusion a) and Drift b) components for the solar cell model CdS/CdSe. The value for  $W$  was set at  $0.56\mu\text{m}$  in order to estimate the diffusion component.

The short circuit current for each model and each layer thickness presented was computed. The calculations were made considering the losses generated by the optical transmission and reflection presented in Fig. 7 and using Equation (12). As mentioned before these calculations were made under de AM 1.5 Standard. For the CdS/PbS model the maximum (absolute) value corresponding the short circuit current density was  $J_{sc}=31.2\text{ mA/cm}^2$ ,  $J_{sc}=16.6\text{ mA/cm}^2$  for the CdS/CdTe design, and  $J_{sc}=17.6\text{ mA/cm}^2$  for the CdS/CdSe type. The similarity of JSC between the CdTe and the CdSe models is due to the closeness of the IQE values for the two, which affects directly the current because of the losses at the collection of charge carriers in the solar cell.

Once  $J_{sc}$  and  $J_d$  were calculated is relatively easy to obtain the J-V for each heterostructures under study. In Figs. 11-13 a) it can observe the curve with a  $V_{oc}$  from 0 to 0.45 V, an electron lifetime  $\tau_n = 10^{-9}$  seconds and a temperature of  $T=300\text{ K}$ . Then the fill factor is computed by the MMS using Equation (21) in order to obtain later the maximum power output of the solar cells. From Tables 2-4, it can be seen that the FF remains basically constant around 0.77 and 0.78. Fill factor can be increased depending on the material resistivity, and by increasing the carrier lifetime [18]. On the other hand, Figs. 11-13 b) shows the maximum output density for the solar cells in function of the applied Voltage. The maximum power density was presented at  $d=2\mu\text{m}$  for all three studies. Being  $P=0.010\text{ W/cm}^2$  at 0.35 V for the CdS/PbS,  $0.005\text{ W/cm}^2$  at 0.37 V for the CdS/CdTe, and  $0.006\text{ W/cm}^2$  at 0.38 V.

Finally, the efficiency is calculated by the MMS using Equation (22) giving a minimum ultimate efficiency ( $\eta$ ) of 7.52, 2.43, and 2.98% for PbS, CdTe, and CdSe active layers at  $d=0.5$

$\mu\text{m}$ , respectively. The maximum values were 10.24, 5.69, and 6.33% for the same order with  $d=2 \mu\text{m}$ .

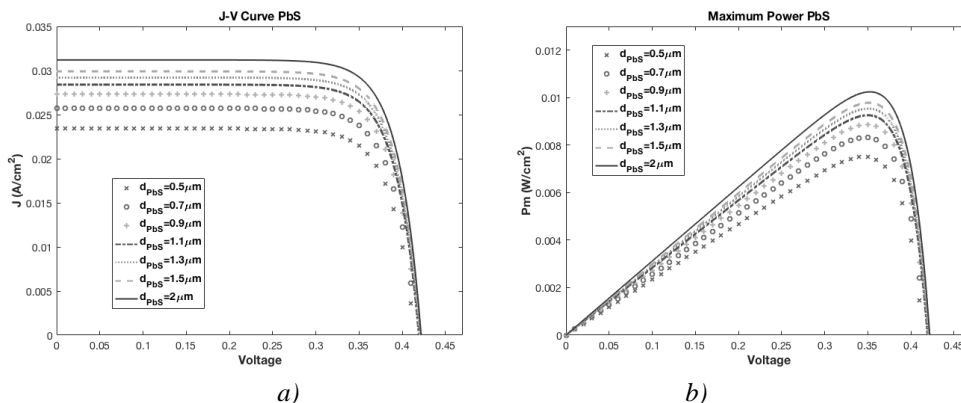


Fig. 11. J-V curve a) and max power density output b) for PbS.

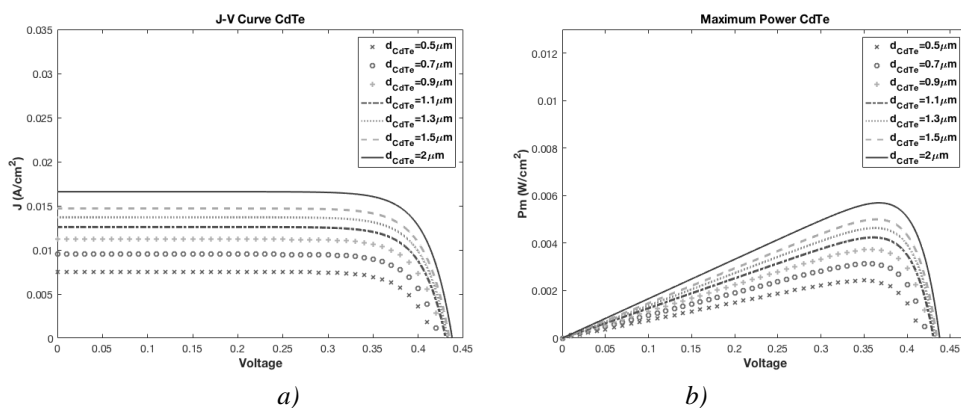


Fig. 12.- J-V curve a) and max power density output b) for CdTe.

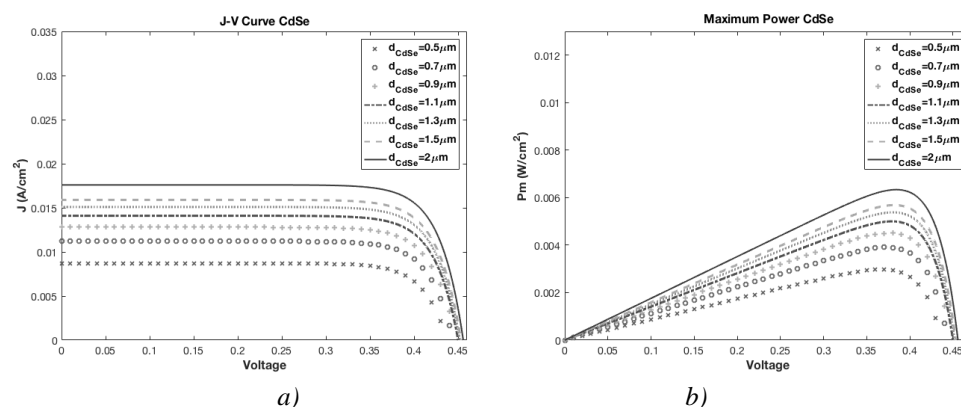


Fig. 13. J-V curve a) and max power density output b) for CdSe.

Table 2, Table 3, and Table 4 show the short circuit current density ( $J_{sc}$ ), Open Circuit Voltage ( $V_{oc}$ ), Maximum Power ( $P_m$ ), Maximum Voltage ( $V_m$ ), Maximum Current Density ( $J_m$ ), fill factor (FF), and characteristic resistance ( $R_{ch}$ ) for each case. The maximum value for the ultimate efficiency corresponds to the CdS/Pbs model, getting 10.24% for a thickness of the active layer of  $2 \mu\text{m}$ .

On the other hand, the minimum value for  $\eta$  recorded corresponds to the CdTe combination with 2.43% for a thickness of 0.5  $\mu\text{m}$ . The characteristic resistance ( $R_{ch}$ ) is obtained by  $R_{ch} = V_m/J_m$

Table 2. Ultimate efficiency ( $\eta$ ) for the modeled heterostructure at different PbS active layer thickness ( $d$ ).

CdS/PbS								
$d$ ( $\mu\text{m}$ )	$J_{sc}$ ( $\text{A}/\text{cm}^2$ )	$V_{oc}$ (V)	$P$ ( $\text{W}/\text{cm}^2$ )	$V_m$ (V)	$J_m$ ( $\text{A}/\text{cm}^2$ )	FF	$\eta$ (%)	$R_{ch}$ ( $\Omega$ )
0.5	-0.0234	0.4143	0.00752	0.3458	0.02174	0.775	7.52	17.3
0.7	-0.0257	0.4167	0.008318	0.3484	0.02387	0.776	8.32	15.17
0.9	-0.0273	0.4183	0.008875	0.3501	0.02534	0.777	8.88	14
1.1	-0.0284	0.4193	0.00926	0.3501	0.02644	0.777	9.26	13
1.3	-0.0292	0.42	0.00954	0.3518	0.02711	0.777	9.54	12.66
1.5	-0.0299	0.4206	0.009786	0.3519	0.02780	0.778	9.79	12.47
2	-0.0312	0.4217	0.01024	0.3553	0.02882	0.778	10.24	12.21

Table 3. Ultimate efficiency ( $\eta$ ) for the modeled heterostructure at different CdTe active layer thickness ( $d$ ).

CdS/CdTe								
$d$ ( $\mu\text{m}$ )	$J_{sc}$ ( $\text{A}/\text{cm}^2$ )	$V_{oc}$ (V)	$P$ ( $\text{W}/\text{cm}^2$ )	$V_m$ (V)	$J_m$ ( $\text{A}/\text{cm}^2$ )	FF	$\eta$ (%)	$R_{ch}$ ( $\Omega$ )
0.5	-0.0075	0.4169	0.00243	0.3493	0.0070	0.7772	2.43	50.21
0.7	-0.0095	0.4232	0.00313	0.3553	0.0088	0.7785	3.13	40.33
0.9	-0.0112	0.4275	0.00373	0.3588	0.0104	0.7790	3.73	34.51
1.1	-0.0126	0.4305	0.00420	0.3622	0.0116	0.7743	4.20	31.24
1.3	-0.0137	0.4326	0.00463	0.3641	0.0127	0.7812	4.63	28.63
1.5	-0.0147	0.4344	0.00500	0.3648	0.0137	0.7830	5.00	26.62
2	-0.0166	0.4376	0.00569	0.3674	0.0155	0.7833	5.69	23.72

Table 4. Ultimate efficiency ( $\eta$ ) for the modeled heterostructure at different CdSe active layer thickness ( $d$ ).

CdS/CdSe								
$d$ ( $\mu\text{m}$ )	$J_{sc}$ ( $\text{A}/\text{cm}^2$ )	$V_{oc}$ (V)	$P$ ( $\text{W}/\text{cm}^2$ )	$V_m$ (V)	$J_m$ ( $\text{A}/\text{cm}^2$ )	FF	$\eta$ (%)	$R_{ch}$ ( $\Omega$ )
0.5	-0.0087	0.4374	0.00298	0.3683	0.0081	0.7831	2.98	45.52
0.7	-0.0112	0.4439	0.00391	0.3744	0.0104	0.7865	3.91	35.85
0.9	-0.0128	0.4474	0.00451	0.3769	0.0120	0.7875	4.51	31.50
1.1	-0.0141	0.4499	0.00500	0.3787	0.0132	0.7882	5.00	28.68
1.3	-0.0151	0.4517	0.00538	0.3813	0.0141	0.7888	5.38	27.02
1.5	-0.0159	0.4530	0.00568	0.3821	0.0149	0.7886	5.68	25.70
2	-0.0176	0.4556	0.00633	0.3848	0.0165	0.7894	6.33	23.39

#### 4. Conclusions

A mathematical modeling was implemented in order to study and compare the parameters that most affect the ultimate efficiency in solar cell structures. Three solar cell heterostructures were modeled based on CdS (n-type window layer), and substituting the active p-layer for PbS, CdTe, and CdSe on each simulation.

Study was based on the calculation for space charge region length, spectrum transmission, absorption, internal quantum efficiency, short circuit current density, dark current density, fill factor, maximum power density output, and ultimate efficiency for the three heterostructure solar cells. Studies were made considering the losses generated by the reflection and absorption through all the layers.

The results indicate that one of the most associated parameters with the ultimate efficiency is the uncompensated donor and acceptor compensations, since this value is highly related to the depletion layer length, which is also a critical parameter for the IQE. The results also show that the thickness of the active layer plays an important role.

From the ultimate efficiency obtained by the MMS one can tell that by under same conditions, the solar cell composed by the CdS/PbS structure gets a higher value in comparison to the other two models. For the PbS structure a maximum efficiency of  $\eta=10.24\%$  against  $\eta=5.69\%$  for CdTe and  $\eta=6.33\%$  for CdSe. Obtained values are similar to efficiencies previously reported in literature [27]. The improvement of the fill factor can directly modify the efficiency of the solar cell; this value is affected by the recombination current in the charge space region of the pn junction. Low recombination current yields to a higher squareness of the FF.

The maximum values were obtained under the following conditions: thickness of the front contact layer (ITO)=150 nm, thickness of the window layer (CdS)=150 nm, thickness of the active layers (PbS, CdTe, and CdSe) =2  $\mu\text{m}$ ,  $\tau=10$  nS,  $W_{\text{PbS}}= 0.28$   $\mu\text{m}$ ,  $W_{\text{CdTe}}= 0.26$   $\mu\text{m}$ ,  $W_{\text{CdSe}}= 0.56$   $\mu\text{m}$  and surface recombination velocity  $S=10^7$  cm/s.

## References

- [1] M. A. Green, K. Emery, Y. Hisikawa, W. Warta, E. D. Dunlop, *Prog. Photovoltaics* **23**, 1 (2015).
- [2] Russell M. Geisthardt, Marko Topic, James R. Sites, *IEEE Journal of Photovoltaics* **5**(4), 1217 (2015).
- [3] Standard Tables for Reference Solar Spectral Irradiances: Direct Normal and Hemispherical on 37° Tilted Surface, ATSM G173-03, 2012.
- [4] T. A. Gessert, S.-H. Wei, J. Ma, D. S. Albin, R. G. Dhere, J. N. Duenow, D. Kuciauskas, A. Kanevce, T. M. Barnes, J. M. Burst, W. L. Rance, M. O. Reese, H. R. Moutinho, *Solar Energy Materials & Solar Cells* **119**, 149 (2013).
- [5] Martin A. Green, Keith Emery, Yoshihiro Hishikawa, Wilhelm Warta, Ewan D. Dunlop, *Progress in Photovoltaic Volume* **21**(1), 1 (2013), <https://doi.org/10.1002/pip.2352>.
- [6] C. Sah, R. N. Noyce, W. Shockley, *Proceedings of the IRE* **45**(9), 1228 (1957).
- [7] The physical properties of glass. Dennis Glyn Holloway, Vol. 24 Wykeham science series, Wykeham Publications, 1973.
- [8] *Semiconductor Material and Device Characterization*. Dieter K. Schroder, 3rd Edition. Jun 2015, Wiley-IEEE Press.
- [9] E. F Schubert, 2004. <https://www.ecse.rpi.edu/~schubert/Educational-resources/Materials-Refractive-index-and-extinction-coefficient.pdf>
- [10] T. M. Bieniewski, S. J. Czyzak, *J. Opt. Soc. Am.* **53**, 496 (1963)
- [11] Mohamed, Hussein, *Journal of Applied Physics* **113**, 10.1063/1.4794201, 2013.
- [12] Madelung, O. ED - Rössler, U., M. Schulz, "Lead sulfide (PbS) optical properties, dielectric constants," M. PY - 1998 DA - 1998// BT - Non-Tetrahedrally Bonded Elements and Binary Compounds I SP - 1 EP - 6 PB - Springer Berlin Heidelberg CY - Berlin, Heidelberg AB - This document is part of Subvolume C 'Non-Tetrahedrally Bonded Elements and Binary Compounds I' of Volume 41 'Semiconductors' of Landolt-Börnstein - Group III Condensed Matter. SN - 978-3-540-31360-1 UR - [https://doi.org/10.1007/10681727\\_881](https://doi.org/10.1007/10681727_881) DO - 10.1007/10681727\_881 ID - ref1
- [13] Y. Fedorenko, J. Major, A. Pressman, L. Phillips, K. Durose, *MRS Advances* **1**(14), 937016). doi:10.1557/adv.2016.69.
- [14] Todd D. Krauss, Louis E. Brus, *Materials Science and Engineering: B*, ISSN: 0921-5107, **69**, 289000).

- [15] L. A. Kosyachenko, E. V. Grushko, O. L. Maslyanchuk, X. Mathew, 33rd IEEE Photovoltaic Specialists Conference, San Diego, CA, USA, 1 (2008).
- [16] F. A. Lindholm, J. G. Fossum, E. L. Burgess, *IEEE Transactions on Electron Devices* **26**(3), 165 (1979), doi: 10.1109/T-ED.1979.19400.
- [17] H. A. Mohamed, *Solar Energy* **108**, 360 (2014).
- [18] Kosyachenko, Leonid, V. Grushko, E. *Semiconductors* **44**, 1375 (2010).
- [19] L. A. Kosyachenko, T. I. Mykytyuk, I. M. Fodchuk, O. L. Maslyanchuk, O. S. Martinez, E. R. Perez, X. Mathew, *Solar Energy* **109**, 144 (2014).
- [20] <http://www.earthtechling.com/2012/01/first-solar-sets-cdte-module-efficiency-mark/>
- [21] *Colour and the optical properties of materials*, Richard J. D. Tilley, June 2011. John Wiley & Sons, Ltd.
- [22] *Semiconductor Physical Electronics*. Sheng S. Li. 2006 2nd Ed. Springer-Verlag New York.
- [23] *Optical Processes in Semiconductors*. Jacques I. Pankove. Courier Corporation, 1975.
- [24] *Elementary Processes in Organic Photovoltaics*. Karl Leo. 2017, Springer International Publishing.
- [25] *Exciton Recombination in the Fullerene Phase of Bulk Heterojunction Organic Solar Cells*, George Frederick Burkhard. April 2011. Stanford University.
- [26] Wu, Kaifeng et al., *Chemical Science* **6**(2), 1049 (2015), PMC. Web. 17 Sept. 2018.
- [27] K. W. Mitchell, A. L. Fahrenbruch, R. H. Bube, *Journal of Applied Physics* **48**(10), 4365 (1977). <https://doi.org/10.1063/1.323429>.